Influence of Molecular Features on the Tackiness of Acrylic Polymer Melts

Hamed Lakrout[†] and Costantino Creton*

Laboratoire de Physicochimie Structurale et Macromoléculaire, Ecole Supérieure de Physique et de Chimie Industrielles, Paris, France

Dongchan Ahn[†]

Department of Chemical Engineering, Northwestern University, Evanston, Illinois 60208-3108

Kenneth R. Shull

Department of Materials Science and Engineering, Northwestern University, Evanston, Illinois 60208-3108

Received November 28, 2000; Revised Manuscript Received July 18, 2001

ABSTRACT: The effects of molecular weight and acrylic acid content on the adhesive properties of a series of monodisperse poly(*n*-butyl acrylate) materials have been investigated. The short-time adhesion, or "tackiness", of these model pressure-sensitive adhesives was quantified by performing probe-tack experiments. These experiments consist of a bonding phase, where a flat punch is brought into contact with a PnBA layer, and a subsequent debonding phase, where the probe is pulled away from the surface. The debonding process was separated into three distinct deformation mechanisms: (1) the appearance of cavities throughout the adhesive layer; (2) lateral growth of these cavities within the plane of the adhesive layer; (3) the formation and eventual failure of a fibrillar structure as the adhesive is extended in the direction of the applied tensile load. Cavitation depends primarily on the elastic character of the adhesive, but the lateral cavity growth and extensional mechanisms are strongly affected by the ability of the adhesive to flow during the time scale of the experiment. The nature of these processes was determined by an effective Deborah number, defined as the terminal relaxation time of the polymer multiplied by the initial strain rate imposed during the debonding process.

1. Introduction

Acrylic polymers are often used as pressure-sensitive adhesives (PSAs) because of their low glass transition temperature and low plateau modulus.[1] Acrylic polymers used in actual adhesive applications are often highly branched or lightly cross-linked and have a very broad molecular weight distribution, with a rheological response that is characteristic of a polymer gel. The complicated molecular structures obtained from standard commercial polymerization processes make it very difficult to relate the adhesive performance to the molecular features of the adhesive. In fact, little is known about the precise role of specific molecular parameters, such as the molecular weight, the molecular weight distribution, gel content, or presence of associating groups on the overall adhesive properties. Obviously, since these molecular features have a profound influence on the deformation behavior of a polymer, there should be a substantial effect on the adhesive properties as well.

Studies with acrylic pressure-sensitive adhesives with a broad molecular weight distribution have provided an important starting point in understanding the relationship between molecular structure and adhesive properties. In studies utilizing a custom-designed probe-tack instrument, Zosel showed that acrylic PSAs deform to high extensions via the formation of a fibrillar structure. He showed in particular that the average molecular weight between entanglements (M_e) is a crucial parameter in the formation of such a structure and that a high value of M_e is a prerequisite for fibril formation.[2] Other studies have shown the influence of the molecular weight on standard performance measures such as tack, peel strength, and shear resistance.[3,4] The main result is that peel and tack energies are highest for an intermediate molecular weight, while the shear resistance increases continuously with increasing molecular weight. However, these studies were all performed with samples with broad molecular weight distributions. Because the detailed debonding mechanisms of PSAs are only beginning to be understood, the analysis of these experimental results was limited primarily to a correlation between the property of interest (shear resistance, tack, etc.) and the average molecular weight. A series of recent theoretical and experimental advances have now shed some light on the details of the mechanisms occurring at the microscopic level when a PSA film is detached from a substrate.[5−9] For this reason it is now possible to investigate the role of the molecular structure of the polymer, not only on the final performance of the adhesive but also on the details of the separation process.

Axisymmetric probe-tack geometries, where a hemispherical or flat punch is brought into contact with an adhesive layer and then pulled away from the surface, are well-suited for studies of pressure-sensitive adhesives. Spherical probes are most useful when the dimensions of the contact area between the indenter and the adhesive are not substantially larger than the

[†] Current address: Dow Corning Corporation, Midland, MI 48686-0994.

* To whom correspondence should be addressed. E-mail Costantino.Creton@espci.fr.

10.1021/ma0020279 CCC: $20.00 © 2001 American Chemical Society
Published on Web 09/07/2001

Table 1. Characterization of the Model Acrylic Polymers

sample	M_w (kDa)	M_n (kDa)	M_w/M_n	T_g (°C)	AA content (mol frac)	τ_d at 20 °C (s)	h_0 (μm)
PnBA-AA-860	1094	860	1.27	−47	0.013	3100	95
PnBA-M-860	1094	860	1.27	−48	0	1570	80
PnBA-AA-300	350	300	1.17	−47	0.044	620	93
PnBA-AA-180	211	183	1.15	−47	0.025	41	100
PnBA-M-180	211	183	1.15	−48	0	6.2	90
PnBA-AA-100	130	100	1.3	−51	*b*	35	150
PEHA-Lat	300[a]	100[a]	3[a]	−57	0		75
PEHA-AA-Lat	300[a]	100[a]	3[a]	−55	0.067		75

[a] Molecular weight data for PEHA-Lat and PEHA-AA-Lat correspond to the sol fraction of the individual latex particles. The gel fraction for these particles was 0.7. [b] Not measured.

adhesive thickness. Provided that the adhesive is sufficiently elastic, failure occurs adhesively as the contact radius shrinks, and a quantitative adhesive failure criterion can be obtained.[8] By using a suitably aligned flat probe (actually the circular end of a cylindrical punch), it is possible to obtain contact radii that greatly exceed the adhesive thickness. In this case the adhesive is highly confined, as in most practical applications, and the mechanics are completely different than for the less-confined case.[6] Because a uniform strain is imposed across a large region of the adhesive, the evolution of debonding as the strain increases can be studied, and a much more detailed understanding of the debonding mechanisms can be obtained than is possible with a traditional peel test. For a peel test the measured force is a superposition of contributions from portions of the adhesive near the peel front that are subjected to a continuous distribution of strains.[10,11] In effect, probe tests can give the entire stress−strain curve of the adhesive, whereas peel tests only give the integral of this curve.

In the present study we utilize an instrumented probe tack apparatus to study the effects of molecular weight and acrylic acid content on the adhesion of monodisperse poly(*n*-butyl acrylate) to the flat end of a cylindrical stainless steel punch. The effects of these variables on the different mechanisms of adhesion are studied individually and are compared to the behavior of a traditional acrylic PSA with a broad molecular weight distribution. In the following Experimental Section, we describe the synthesis and characterization of the polymers used in these experiments, in addition to the probe-tack experiment itself. In the Results section we define the three fundamental deformation mechanisms that describe the debonding process and show how each of these mechanisms is affected by the molecular features of the adhesive. Some unifying ideas for understanding these results are given in the Discussion section.

2. Experimental Section

2.1. Synthesis of Model Acrylic Polymers. The monodisperse acrylic adhesive was poly(*n*-butyl acrylate) (PnBA) derived from a parent poly(*tert*-butyl acrylate) (PtBA).[12−14] Precursors of PtBA were synthesized by living anionic polymerization at −78 °C in tetrahydrofuran (THF). PtBA precursors of four different molecular weights were obtained by varying the relative amount of monomer and initiator added to the solution. *sec*-Butyllithium was reacted with diphenylethylene to form the initiator, and the polymerization was done in the presence of lithium chloride in order to narrow the molecular weight distributions of the polymers. Estimated molecular weights of these polymers were determined by gel permeation chromatography (GPC) in THF and are reported in Table 1 in terms of values obtained from a calibration with polystyrene standards. The polydispersity indices (M_w/M_n) of the PtBA

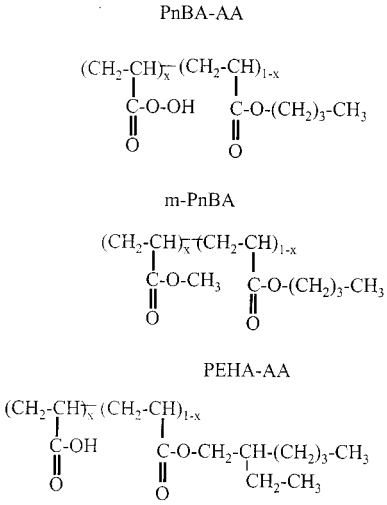

Figure 1. Chemical structures of the model acrylic pressure-sensitive-adhesives: (a) PnBA-AA; (b) PnBA-M; (c) PEHA-AA.

samples were between 1.1 and 1.3. The GPC results are used primarily to give an indication of the polydispersity of the polymers, since Klein et al. have shown that for molecular weights that exceed 100 000, the use of polystyrene standards underestimates the true molecular weight of PtBA.[15]

The PtBA was converted into PnBA by acid-catalyzed transalcoholysis in *n*-butyl alcohol, with *p*-toluenesulfonic acid as the catalyst.[14] GPC measurements after the transalcoholysis confirmed that the molecular weight distribution of the precursors was not affected by the transformation. Because the replacement of some of the *tert*-butyl side groups by carboxylic groups (COOH) is nearly unavoidable, the product of the transalcoholysis reaction is in fact a copolymer of *n*-butyl acrylate and acrylic acid rather than a homopolymer of PnBA, with a chemical structure shown in Figure 1a. These polymers are designated as PnBA-AA-XX, where XX is the molecular weight in kg/mol. As shown in Table 1, the mole fractions of acrylic acid in the polymers are relatively low (less than 0.05). The qualitative features of the PnBA rheology are not substantially affected by the incorporation of the acrylic acid. Rather, the net effect of the acid groups on the rheological properties is to increase all of the longer relaxation times of the polymer by a constant factor, resulting in an increase in the terminal relaxation times of the polymers.[14]

Since the adhesive properties of the polymers were expected to be sensitive to the presence of acrylic acid, we methylated two of these copolymers, giving polymers with the chemical structure shown in Figure 1b. This process consists of the substitution of acrylic acid groups by methyl groups (CH_3) by mixing the PnBA-AA with diazomethane in a THF solution. Diazomethane had been previously obtained from the reaction of nitrosomethylurea in a potassium hydroxide aqueous solution.[16] Proton NMR measurements showed that the substitution of acrylic acid groups actually took place, and from the ester groups, the amount of acrylic acid present in the PnBA-AA could be estimated.[14] In contrast to the acrylic acid, the methyl groups are not expected to substantially affect the rheological or adhesive properties of the PnBA. Portions of

PnBA-AA-180 and PnBA-AA-860 were methylated, giving polymers that are referred to as PnBA-M-180 and PnBA-M-860.

The polydisperse acrylic adhesives with a broad distribution of relaxation times were based on poly(ethylhexyl acrylate). These materials were made by emulsion polymerization and delivered as a latex emulsion with a concentration of solids of 50 wt % (Elf-Atochem, France). The individual latex particles had a gel fraction of 0.7. The sol fraction, characterized by gel permeation chromatography, had a weight-average molecular weight of about 300 kg/mol and a polydispersity index of 3. To study the effects of acrylic acid on the adhesive behavior of these materials, two different latexes were used. One sample was a poly(ethylhexyl acrylate) homopolymer and is referred to in our notation as sample PEHA-Lat. The other sample was a copolymer of poly(ethylhexyl acrylate) and acrylic acid and is referred to as PEHA-AA-Lat. The weight fraction of acrylic acid content for this sample was 0.025, corresponding to a mole fraction of 0.07. The chemical structures of the PEHA polymers are shown in Figure 1c. The adhesive behavior of these materials has been described in detail in a previous publication.[7] Only a few results from this polymer are included here, in those cases where comparison to the results obtained from the monodisperse PnBA (with a well-defined terminal relaxation time) samples is useful.

2.2. Rheological Characterization. The glass transition temperatures (T_g) of the PnBA samples were determined by differential scanning calorimetry (DSC) at a heating rate of 10 °C/min. Glass transition temperatures for the PnBA samples were -49 ± 2 °C and were not significantly affected by the relatively low levels of acrylic acid present in some of the polymers. Dynamic shear moduli were performed with a parallel plate rheometer (RDA II, Rheometrics) at frequencies between 10^{-1} and 100 Hz and at temperatures between -50 and 80 °C. Samples for the rheological studies were prepared by slow evaporation of the solvent (for the PnBA) or water (for the lattices) from samples that had been placed in a Teflon mold. The parallel disks were 8 mm in diameter. A master curve was obtained using a temperature-dependent shift factor, a_T, which can be expressed in the following form:

$$\log(a_T) = A + \frac{B}{T - T_\infty} \tag{1}$$

For PnBA the experimentally determined shift factors were consistent with previously published values of 770K for B and -105 °C for T_∞.[14] The constant A depends on the reference temperature of interest and is equal to -6.16 for a reference temperature of 20 °C. Representative data corresponding to this reference temperature are plotted in Figure 2. For the linear PnBA polymers a well-defined plateau modulus of about 0.15 MPa is obtained, corresponding to a molecular weight between entanglements of 22 kg/mol. The terminal relaxation time, τ_d, for these polymers was defined as $2\pi/\omega_c$, where ω_c is the crossover angular frequency where G' and G'' are equal to one another. These relaxation times are listed in Table 1.

Temperature shift factors used for the PEHA data over the measured temperature range (-50 to 50 °C) were described by eq 1 with $B = 860$ and $T_\infty = -124$ °C, giving $A = -5.97$ at the reference temperature of 20 °C. As illustrated in Figure 2, the dynamic mechanical data for these materials are characteristic of highly branched polymer gels, with a broad distribution of relaxation times and a power-law dependence on frequency for both G' and G''. A single characteristic relaxation time cannot be defined for these materials.

2.3. Probe-Tack Test of Adhesion. Thin films of PnBA were spread with a doctor blade from a butanol solution on standard precleaned microscope glass slides. Similar procedures were used to prepare adhesive layers from the PEHA latex suspensions. The samples were dried at 70 °C for 4 h under low vacuum. After 1 h at steady temperature conditions (-10, 23, or 60 °C), a flat punch was brought into contact with the adhesive layer at a velocity of 30 μm/s. The flat probe was the end of a stainless steel cylinder with a 1 cm diameter. This flat surface had been sand-blasted, producing a roughened surface with Gaussian distribution of asperity heights, with an average height of 1.2 μm. The punch was held at a fixed

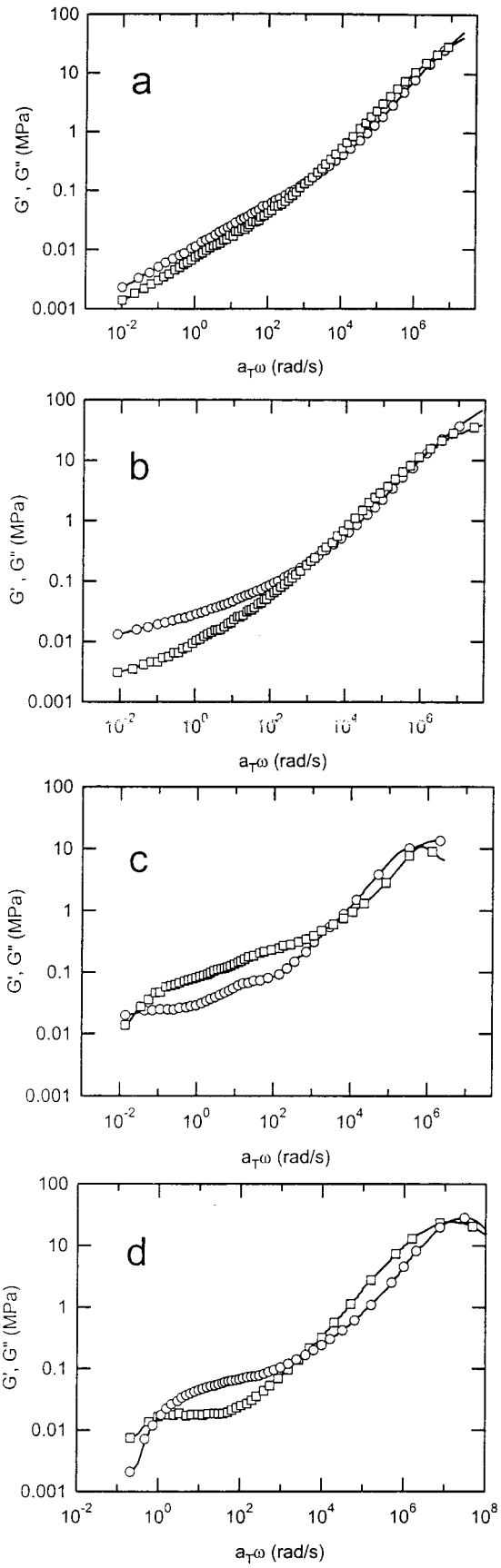

Figure 2. Dynamic mechanical spectra for different model adhesives: (a) PEHA-LAT, (b) PEHA-LAT-AA, (c) PnBA-M-180, (d) PnBA-AA-180. ○, G'; □, G''.

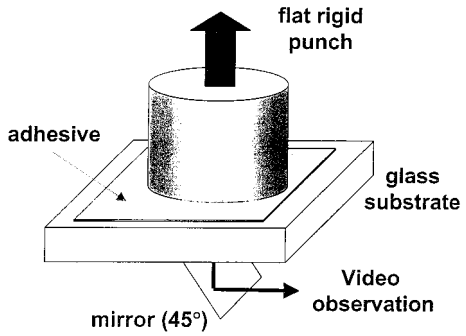

Figure 3. Schematic of the flat probe tack test.

position for a contact time of $t_c = 1$ s and subsequently removed at a constant debonding velocity (V_{deb}) that was varied from 1 to 10^4 μm/s for different tests. The complete experimental setup is described in more detail elsewhere[7] and is shown schematically in Figure 3. Events occurring at the adhesive/probe interface were recorded with a CCD camera in PAL format (25 frames/s) and synchronized to the stress−strain curve. With this arrangement we were able to visualize the entire contact area with a resolution of about 100 μm. Values of the maximum area of contact A_0 were determined by inspection of the images obtained in this way.

The average size of the cavities observed during the debonding stage was also obtained through an analysis of the video images. For each experimental condition, representative images of a late stage in the debonding process (when cavities occupy nearly all the area initially bonded) were digitized, and the average area of the cavities was obtained by dividing the total debonded area by the number of cavities which were present.

In the following we will refer to the tensile stress σ as the ratio between the tensile force $F(t)$ and the maximum area of contact A_0 of the probe, $F(t)/A_0$, to σ_{max} as the maximum tensile stress, and to the strain ϵ as the ratio between the displacement of the punch $\delta(t)$ and the initial thickness h_0 of the adhesive layer, $\epsilon(t) = \delta(t)/h_0$. The maximum strain ϵ_{max} is the strain at which the stress decreases to a value that is less than 0.005 MPa. The adhesion energy W_{adh} is defined as the area under the load−displacement curve, normalized by the maximum contact area:

$$W_{adh} = \frac{1}{A_0}\int F(\delta)\,d\delta = h_0\int \sigma(\epsilon)\,d\epsilon \qquad (2)$$

3. Results

3.1. General Description of the Deformation Mechanisms. A typical stress−strain curve is shown in Figure 4, along with representative images taken through the thickness of the adhesive. Previous tack studies undertaken with the flat probe geometry have shown that the debonding of a soft adhesive occurs through a general sequence of mechanisms and that these mechanisms are determined both by the geometry of the test and by the properties of the adhesive.[5,7] These deformation mechanisms for a soft adhesive are as follows, listed in the general order in which they take place.

Mechanism I—Cavitation: formation of cavities at the interface between the probe and the film or inside the film.

Mechanism II—Lateral cavity growth: lateral growth of the cavities in the plane of the film.

Mechanism III—Extensional cavity growth: growth of the cavities in the direction normal to the plane of the film, with eventual formation of a fibrillar structure.

Cavitation (mechanism I) is a consequence of the very confined geometry of the test and is almost always

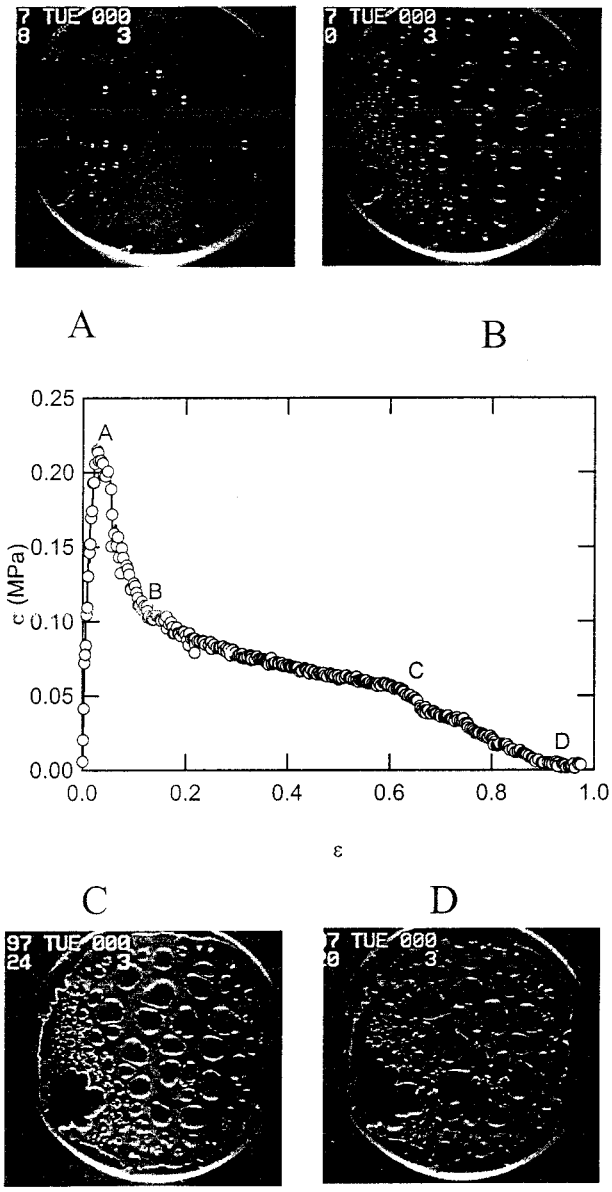

Figure 4. Characteristic tack curve, showing representative images of the adhesive at different times during the test.

observed when the ratio of the punch radius (a) to the original film thickness (h_0) is sufficiently high. The only exceptions among the materials described in this study were the high molecular weight PnBA samples (PnBA-M-860 and PnBA-AA-860). In these samples adhesive failure occurred by the propagation of fingerlike cracks originating at the periphery of the contact area, before the tensile stress required for cavitation was realized. For materials with a strong elastic character the balance between cavitation and this edge crack propagation mechanism is determined by the elastic modulus of the adhesive, the degree of confinement as characterized by a/h_0, and an adhesive failure criterion that can be expressed in terms of a critical energy release rate, G_c.[5] For the high molecular weight PnBA sample, G_c is relatively low and the elastic modulus at the debonding frequency is relatively high. In this case the preexisting crack at the edge of the probe is able to propagate for a lower applied stress than is required for cavitation within the bulk of the adhesive film. We attribute this result to the long relaxation times of this polymer and to the inability of this highly elastic polymer melt to

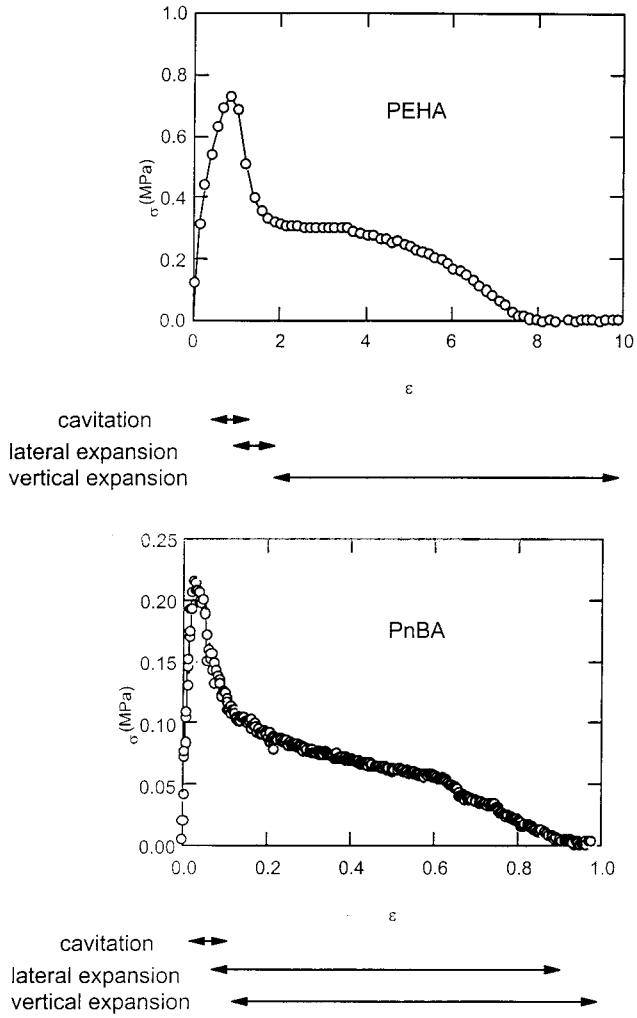

Figure 5. Stress−strain curves showing the regions where different deformation mechanisms are operative, illustrating two types of response: (a) lateral expansion of the cavities followed by extension of a fibrillar structure; (b) simultaneous lateral expansion and extension of the cavities.

form a strong bond with the probe during the bonding phase of the experiment.

Once cavitation occurs, the lateral and extensional growth of these cavities (mechanisms II and III) is dependent on the type of adhesive, temperature, and debonding rate. These mechanisms can be observed directly with the video and are associated with different portions of the stress−strain curve. In some cases the mechanisms proceed sequentially, and the cavities initially grow laterally and then are extended vertically as a fibrillar structure develops. In the absence of strain hardening of the fibrils, the stress remains relatively constant as the fibrils are extended, and a stress−strain curve of the sort shown in Figure 5a is obtained. In other cases there is significant overlap between mechanisms II and III. In these cases the cavities grow simultaneously in the lateral and extensional directions, and the stress continuously decreases after passing through the maximum associated with the cavitation process. This situation corresponds to the stress−strain curve shown in Figure 5b. Note that this division of the debonding process into elementary mechanisms is a necessary feature of our analysis, since molecular characteristics such as the molecular weight and the presence of acrylic acid have a much stronger effect on some mechanisms than on others. In subsequent sections, we consider each of these mechanisms individually.

3.2. Effects of the Bonding Phase and Breakdown of Time−Temperature Equivalence. Each of the deformation mechanisms defined above characterizes the debonding process. In some cases it is important to understand effects associated with the bonding process as well. In our experiments the bonding time, determined primarily by the 1 s hold time between the loading and unloading portions of the test, is independent of the temperature. At low temperatures, this experimental time can be less than the relaxation times associated with the formation of a good bond between the probe and the surface. The time required for the adhesive to conform to the roughness of the probe surface is just one example of a relevant relaxation time.[17,18] For this reason, debonding experiments performed at different temperatures do not necessarily begin with the same initial condition. If bonding between the adhesive and probe surface is not achieved, any mechanism that depends on the adhesive strength of the probe/adhesive interface will be affected. The failure of time−temperature superposition to describe many of the results given below is potentially an artifact associated with the bonding phase of the experiment.

3.3. Mechanism I: Cavitation. After a linear increase of the stress corresponding to the homogeneous deformation of the film, cavities begin to appear. The first cavities appear well before the maximum of stress and are responsible for the nonlinear increase of stress with additional displacement. Nevertheless, most of the cavities appear at a stress that is within 10% of the maximum value. Careful observations at higher magnifications, utilizing a different experimental apparatus, showed that the cavities formed within 5 μm of the interface adhesive/probe interface. For technical reasons these observations were only possible at room temperature. However, very similar pictures obtained at a lower magnification for all the temperatures were consistent with this mechanism. The cavities appeared randomly throughout the area of contact of the flat punch, and their projection on the plane of the interface was approximately circular. The rate of initial growth of the void diameter was estimated at about 1 cm/s, regardless of the conditions of the tests. Cavitation was therefore a high-speed process relative to the punch withdrawal rate. With the exception of the PnBA-AA-860 and PnBA-M-860 samples, this description of the cavitation process applied to all the samples tested, regardless of their particular molecular features.

To illustrate the dependence of the cavitation stress on the debonding velocity, temperature, and molecular features of the polymer, values of the measured maximum stress are plotted as a function of the reduced velocity in Figure 6 for the carboxylated polymers and in Figure 7 for the non-carboxylated polymers. For the range of debonding rates investigated, the maximum stress increased with the debonding rate, as one would expect for a viscoelastic material. To compare the values of the maximum stress for the different samples, the following empirical form of the velocity dependence of σ_{max} is included on each curve:

$$\sigma_{max} = 0.2(a_T V)^{0.15} \quad (3)$$

with σ_{max} in MPa and V in μm/s. As with all of the

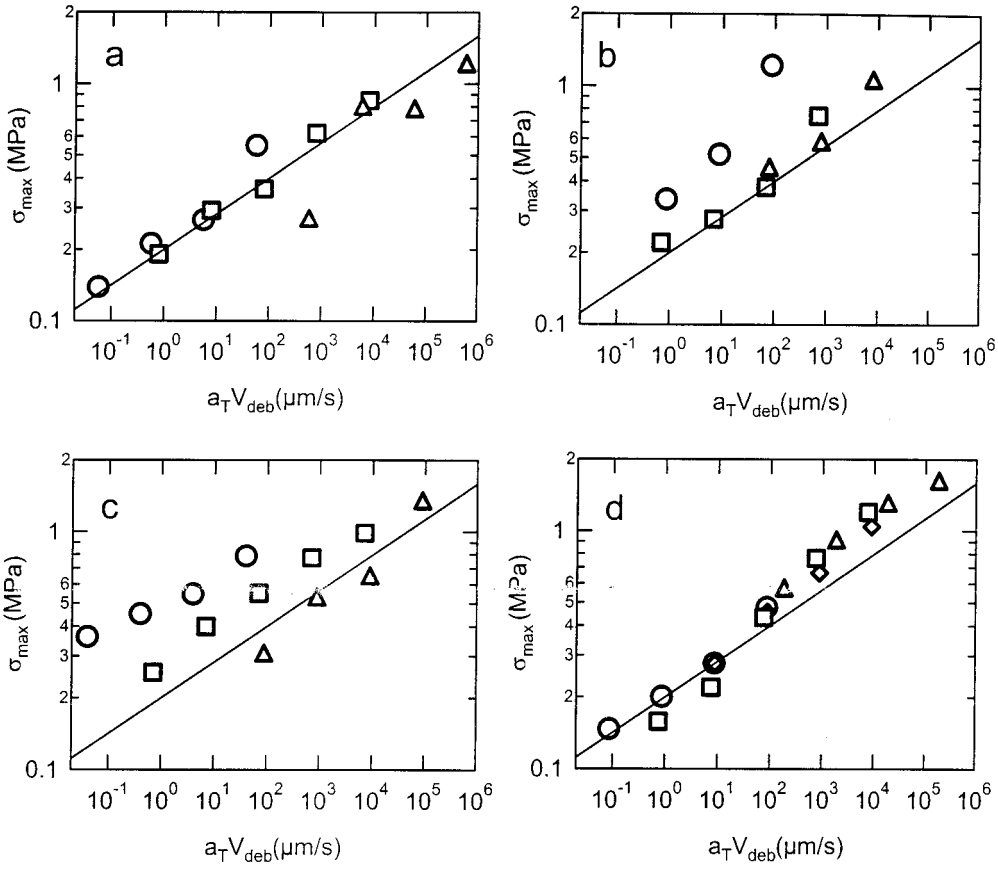

Figure 6. Maximum stress as a function of reduced velocity for carboxylated polymers (at a reference temperature of 20 °C): (a) PnBA-AA-100; (b) PnBA-AA-180; (c) PnBA-AA-300 at −10 °C (△), 23 °C (□), and 60 °C (○). (d) PEHA-AA-LAT at −20 °C (△), 0 °C (◇), 23 °C (□), and 50 °C (○).

results described in this paper, a reference temperature of 20 °C was used. Time−temperature superposition works well for the non-carboxylated polymers, and also for the PEHA latexes, and to some extent for the lowest molecular weight carboxylated PnBA sample. Time−temperature superposition clearly fails to describe the behavior of the higher molecular weight PnBA samples. This result is attributed to imperfect bonding of these polymers at the lower temperatures.

The process of cavity growth in a purely elastic rubber has been studied extensively.[7,19−25] The central theoretical prediction is that an unstable expansion of the cavity should occur when the tensile hydrostatic pressure exceeds the value of Young's modulus, E, of the rubber. Application of these ideas to viscoelastic materials is complicated by the fact that these materials do not have a single well-defined modulus. In our analysis we define an effective frequency, f_{eff}, for the tack test (and the associated angular frequency, ω_{eff}) in the following way:

$$f_{eff} = \omega_{eff}/2\pi = V_{deb}/h_0 \tag{4}$$

and assume that the appropriate modulus is the storage modulus at this effective frequency. To account for the effects of viscous flow, we introduce a Deborah number, defined in general as the product of the strain rate and the relevant relaxation time for flow of the polymer. For the monodisperse PnBA samples, the appropriate relaxation time is the terminal relaxation time, τ_d, which increases roughly with the cube of the molecular weight and which increases by a factor of 5−10 when several mole percent acrylic acid is incorporated in the polymer. The nominal strain rate is given by V_{deb}/h_0, so the Deborah number, De, is given by the following expression:

$$\mathrm{De} = \tau_d a_T V_{deb}/h_0 \tag{5}$$

When using the Deborah number defined by eq 5, it is important to keep in mind that this quantity only describes the actual Deborah number very early in the test, when the imposed strain is low and uniform throughout the material. In the later states of the test, the strain is highly nonuniform, and different regions of the sample are characterized by different "local" Deborah numbers. Nevertheless, when comparing results obtained for tests performed at different debonding rates and temperatures, the effective Deborah number defined by eq 5 remains a useful measure of the overall rate of the test in comparison to the relaxation time of the polymer.

Figure 8a shows $\sigma_{max}/G'(\omega_{eff})$ plotted as a function of the Deborah number for all of the carboxylated PnBA samples. Despite a substantial scatter in the data points, it is apparent that $\sigma_{max}/G'(\omega_{eff})$ is roughly constant (∼5) for De > 1 and greatly increases for smaller values of De. [While this is not apparent from Figure 8a, $\sigma_{max}/G'(\omega_{eff})$ decreases below 5 for the experiments performed on the PnBA-AA-300 and the PnBA-AA-180 at the lowest temperature. This reflects the failure of time−temperature superposition discussed earlier and shown in Figure 6b,c.] A very similar result is found for the methylated polymer (PnBA-M-180, Figure 8b) although the constant value of $\sigma_{max}/G'(\omega_{eff})$ obtained at high values of De is higher than for the carboxylated polymers and more in agreement with the

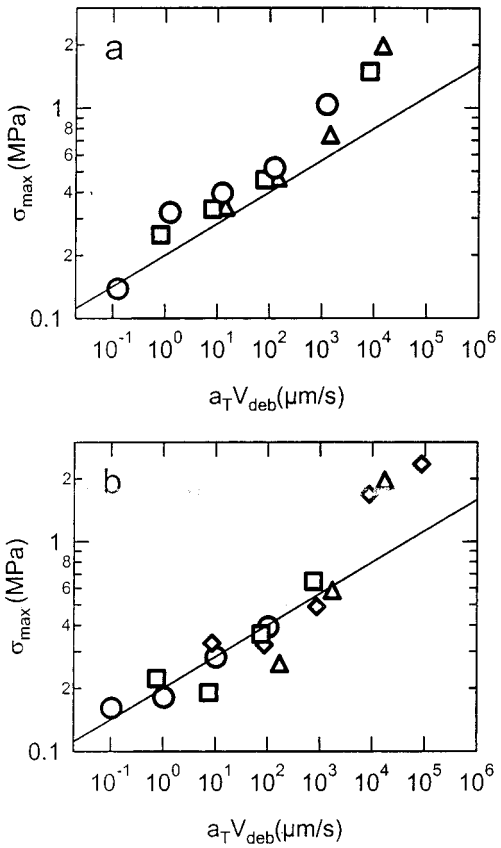

Figure 7. Maximum stress as a function of reduced velocity for noncarboxylated polymers. (a) PnBA-M-180 at −10 °C (△), 23 °C (□), and 60 °C (○). (b) PEHA-AA-LAT at −20 °C (△), 0 °C (◇), 23 °C (□), and 50 °C (○).

results previously obtained for the PEHA latex.[7] The increase of $\sigma_{max}/G'(\omega_{eff})$ at low De is mainly due to the fact that, as the shear modulus can decrease to zero, the critical stress for cavitation cannot decrease below a lower limit given by the outside pressure. If probe-tack experiments were performed at a lower outside pressure, one would expect $\sigma_{max}/G'(\omega_{eff})$ to remain constant for lower values of the Deborah number. The fact that the transition from one regime to the other occurs for De ∼ 1 could be interpreted as a proof that viscous flow plays a major role. In fact, our results can be accounted for by the marked decrease of the elastic component of the shear modulus for De < 1. For values of $G' \sim 0.1$ MPa, the outside pressure is only felt over a small distance near the edge of the probe, and the stress distribution under the probe is essentially flat[6,26] (constant tensile stress under the probe). When G' decreases, the influence of the outside pressure extends over an increasingly larger area of the probe until it is felt over the whole volume of the adhesive film. At that stage, cavitation cannot occur for an average applied stress below the outside pressure.

The results obtained with the monodisperse PnBA samples indicate that the cavitation process is controlled by the *elastic* nature of the adhesive rather than by its *viscous* component. While these concepts were also used to interpret the results obtained with the PEHA latex,[7] the almost identical frequency dependence of G' and G'' for these polymers (see Figure 2a,b) makes it impossible to differentiate between elastic and viscous contributions to the stress.

3.4. Mechanism II: Lateral Cavity Growth. The process of cavity growth within the plane of the adhesive

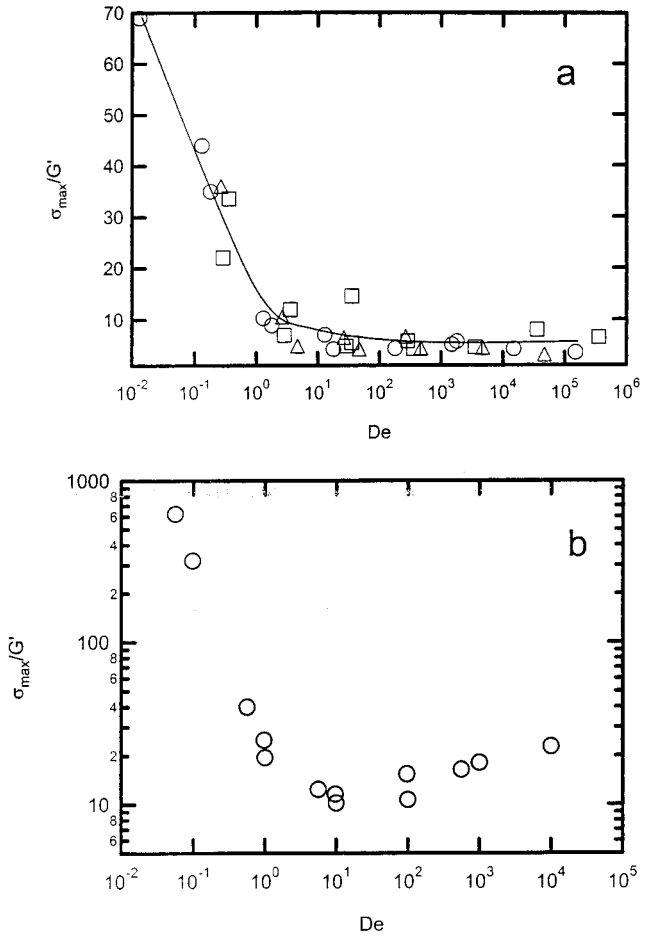

Figure 8. Maximum stress normalized by $G'(\omega_{eff})$ as a function of the Deborah number: (a) (○) PnBA-AA-100; (□) PnBA-AA-180; (△) PnBA-AA-300. (b) PnBA-M-180.

layer is important because it is the link between a flat film with cavities and a fibrillated structure. The process begins when new cavities are nucleated and ends when the walls between cavities have reached a stable size. For most of the tests performed on PnBA samples, the end of the in-plane growth process occurs at strains between 0.5 and 1. For a displacement of the probe of about 100 μm, the cavities can have an average diameter of about a millimeter, in which case the voids must be viewed as thin disks rather than spheres.

The average final size of the cavities generally decreases with increasing molecular weight, an effect that is amplified by reducing the debonding rate or increasing the temperature. Representative results obtained from carboxylated PnBA samples are illustrated in Figure 9. For the polymer with the highest molecular weight (300 kg/mol) a large number of small cavities with circular cross sections are observed. For the polymer with an intermediate molecular weight (180 kg/mol) the cavities are larger and less numerous, but with cross sections that are still essentially circular. For the lowest molecular weight polymer (100 kg/mol) the cavity cross sections are no longer circular and exhibit Saffman−Taylor fingering.

Because cavity growth is determined by a combination of elastic and viscous effects, it is again useful to use the Deborah number to define different experimental regimes. The images shown in Figure 9 correspond to Deborah numbers that increase from 0.18 (top image) to 0.29 (middle image) to 4.8 (bottom image). A more

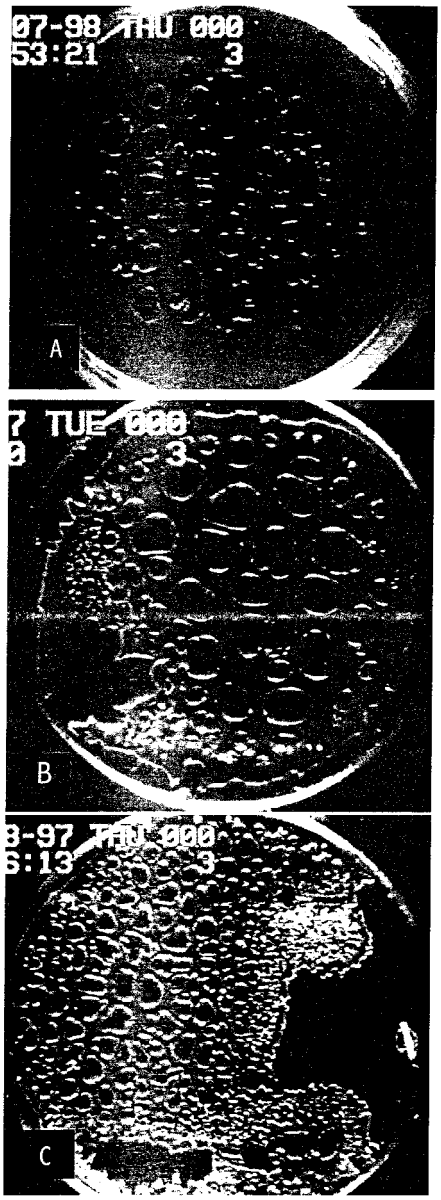

Figure 9. Representative images at the end of the lateral cavity growth phase for the carboxylated PnBA polymers: (A) PnBA-AA-100, De = 0.18; (B) PnBA-AA-180, De = 0.29; (C) PnBA-AA-300, De = 4.8.

extensive correlation between the stable cavity size and the Deborah number is shown in Figure 10. In this figure the average cross-sectional area of a cavity (obtained from analysis of the individual images) is normalized by the square of the adhesive layer thickness and plotted as a function of De. For values of De larger than about 10, there is very little cavity growth, and the final size of the cavities is determined by the elastic stresses that govern cavity nucleation. In this case the average distance between cavities, and the geometrically related average cavity size, are determined by the size of the zone throughout which an individual cavity is able to relax elastic stresses in the surrounding adhesive. The size of this "zone of influence" for the cavity is predicted to scale as $h_0(K/G)^{1/2}$ where K is the bulk modulus of the adhesive.[25,26] Because the stresses are relaxed in this zone, additional cavities are not able to nucleate. The observed cavity sizes of a few times the film thickness in the high De regime are consistent with this picture. At low values of the Deborah number,

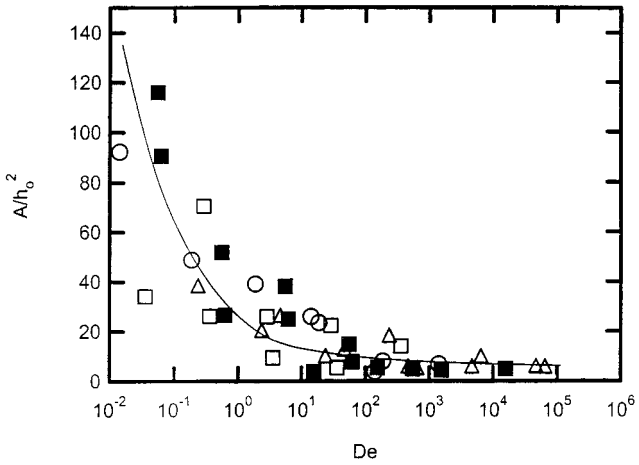

Figure 10. Average projected area of the cavities normalized by the square of the film thickness, as a function of the Deborah number: (○) PnBA-AA-100; (□) PnBA-AA-180; (△) PnBA-AA-300; (■) PnBA-M-180.

larger cavities are obtained for two related reasons. First, the cavities themselves are able to grow by viscous flow. Second, the zone of influence surrounding these cavities is increased in size by relaxation of the stress field.

3.5. Mechanism III: Extension of the Adhesive Material. The final mechanism considered here corresponds to the growth of the cavities in the direction normal to the plane of the interface and to the formation and breakdown of a fibrillar structure. While the mechanisms of lateral and extensional growth are clearly separated for the PEHA materials, these mechanisms occur simultaneously for the PnBA materials, at least for relatively low Deborah numbers. The maximum strain obtained prior to either adhesive or cohesive failure is a useful measure of the final extension of the fibrils formed by the adhesive. This maximum strain is referred to as ϵ_{max} and is defined operationally as the strain at the point where the measured stress falls below 0.005 MPa. This maximum extension is plotted as a function of the Deborah number for the carboxylated PnBA samples in Figure 11a−c. The maximum extension varies strongly with debonding rate and temperature and goes through a maximum at a critical value of the Deborah number. This maximum corresponds to a transition from cohesive fracture to adhesive fracture as De is increased. For all three carboxylated polymers, this transition occurs for 100 < De < 1000. On the other hand, for the PnBA-M-180 sample (Figure 11d), the transition is not observed and occurs for De > 10^4.

For an elastomer, the adhesive failure criterion can be expressed as a relationship between a crack velocity and an applied energy release rate or stress intensity factor.[27] A similar approach can be applied to describe viscoelastic materials as well, although the stress intensity factor gives a more rigorously appropriate failure criterion in this case.[28] This stress intensity factor is conceptually related to the critical stress for adhesive failure defined by Kaelble in his analysis of peel experiments.[10] In our case the velocity dependence of this critical stress can be accounted for by using an "effective" critical stress that depends on the debonding velocity. When this critical stress is exceeded, failure occurs by lateral growth and then coalescence of the cavities via debonding at the probe/adhesive interface.

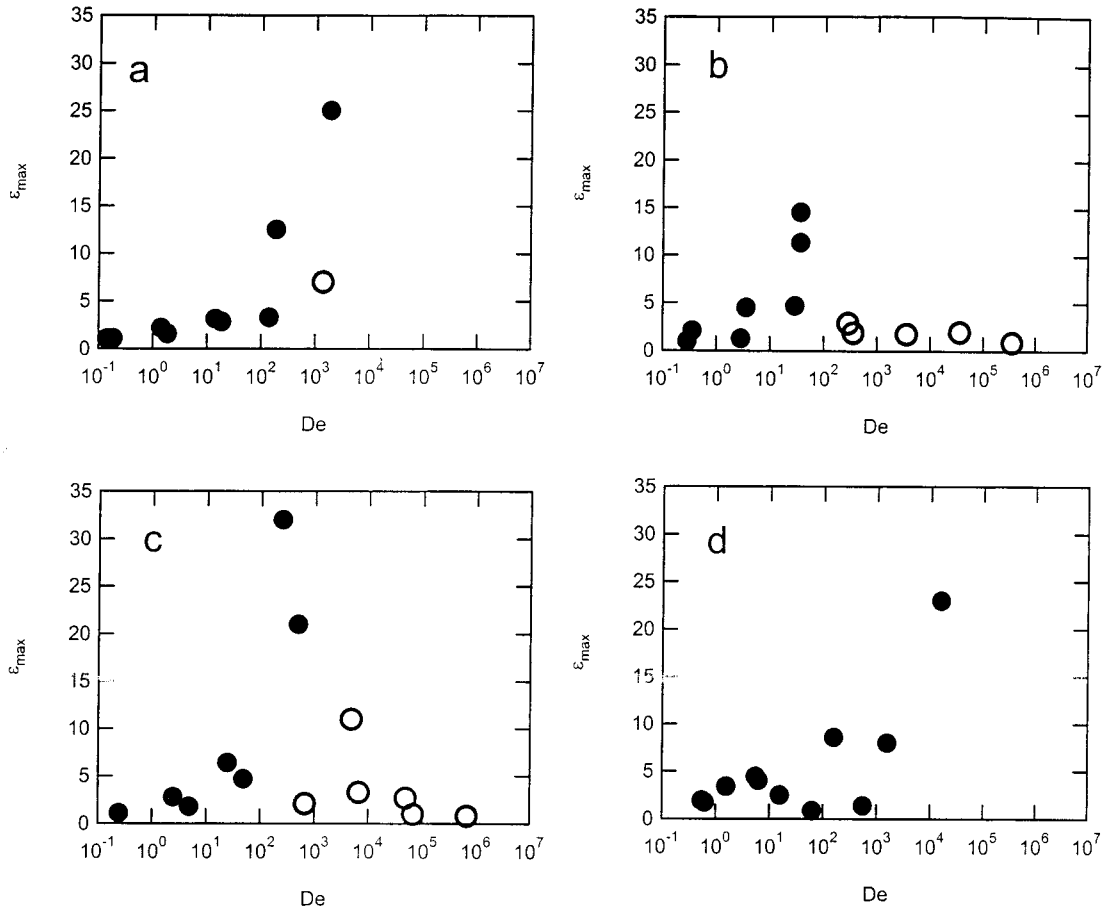

Figure 11. Maximum extension as a function of Deborah number for PnBA samples, showing the transition from cohesive to adhesive failure: (a) PnBA-AA-100; (b) PnBA-AA-180; (c) PnBA-AA-300; (d) PnBA-M-180. (●) Cohesive failure; (○) adhesive failure.

For the PnBA polymers, adhesive failure by this mechanism occurs prior to substantial extensional cavity growth, resulting in a relatively low value of ϵ_{max} and a low overall adhesion energy. The specific location of the adhesive/cohesive transition will depend on the value of this critical stress, but it is interesting to note that the transition occurs at very large Deborah numbers, where at low strains the polymer behaves as a rubbery solid. This result indicates that, in the presence of a suitably large applied stress, chain disentanglement is able to occur over times that are very small in comparison to the terminal relaxation time.

At this point we are in a position to consider the role played by acrylic acid groups in the adhesive process. While fibril failure is still observed at relatively large Deborah numbers for the carboxylated polymers, these Deborah numbers are a factor of 1000 less than the largest Deborah numbers obtained for the methylated polymers (compare parts b and d of Figure 11). This result indicates that acrylic acid groups have a substantial effect on the large-strain extensional properties of the PnBA. These changes are much larger than the changes in the linear viscoelastic properties, since these linear effects are already accounted for in the determination of the Deborah number. In other words, the chain disentanglement process at large strains is 10 000 times faster for the PnBA-M-180 than for the PnBA-AA-180 while the terminal relaxation time is only 8 times lower.

This effect could be due to the presence of a transient network of physical cross-links, which greatly increase the cohesive properties of the polymer and its strain hardening behavior at large strains. This role of the acrylic acid groups could also potentially explain why the cohesive−adhesive transition does not occur precisely at the same value of De for all three carboxylated polymers, since they contain slightly different amounts of AA. A similar qualitative effect had been observed with PEHA gels, but a possible difference in degree of polymer chain branching, due to the different synthesis conditions, made it difficult to attribute unambiguously the different tack behaviors to the presence of acrylic acid.[7]

4. Discussion

While our approach of breaking the debonding process into elementary stages is very informative, it is also useful to relate these processes to more commonly utilized measures of practical adhesion. The parameter that is most closely related to the peel energy is the adhesion energy, W_{adh}. This quantity, given by the integral under the tack curve as defined in eq 2, is plotted in Figure 12a for all three carboxylated PnBA polymers and in Figure 12b for the methylated PnBA polymer as a function of the Deborah number. The lines to guide the eye underline the existence of separate adhesive and cohesive branches of the adhesion energy curves. Similar branches have been observed for peel tests[29−31] and are indicative of a change in the failure mechanism. In the cohesive regime, stresses are typically low and extensions are high, while in the adhesive regime, stresses are high and extensions are low. Note also the high De data points for the PnBA-300-AA polymer (dotted horizontal line) which do not fall on the adhesive branch of the adhesion energy curve. For these

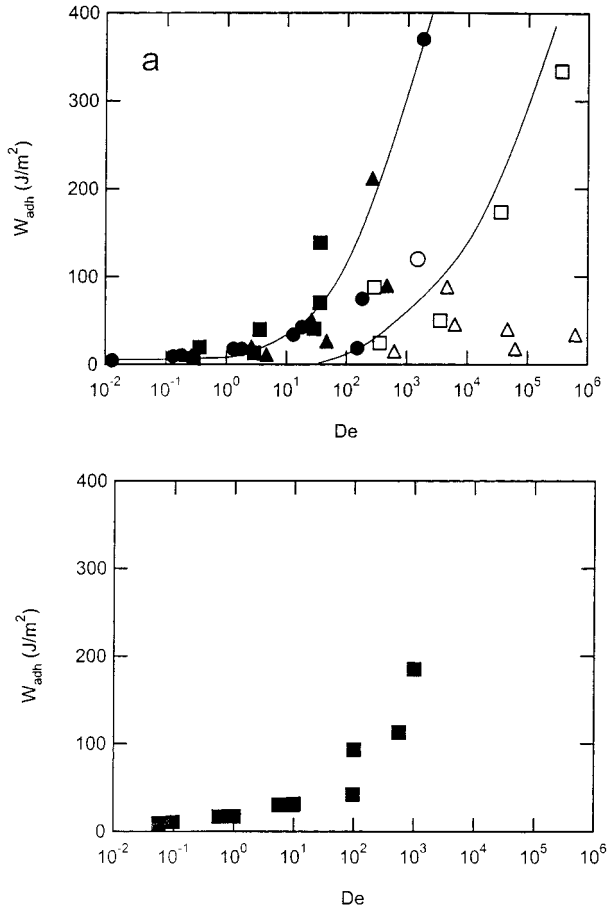

Figure 12. Practical work of adhesion W_{adh} as a function of the Deborah number, showing the adhesive and cohesive branches. (a) (○) PnBA-AA-100; (□) PnBA-AA-180; (△) PnBA-AA-300; (b) (■)PnBA-M-180. In part a filled symbols are representative of a cohesive failure while unfilled symbols are representative of an adhesive failure. The solid lines guide the eye to the cohesive and adhesive branches of the adhesion energy curves.

experimental conditions the adhesion energy was limited by poor bonding and time−temperature superposition failed.

The work of adhesion depends on the maximum stress and on the maximum extension. While these quantities can have different rate dependencies, both are closely related to the viscoelastic properties of the adhesive, as discussed above. The overall adhesion energy can be related to the product of σ_{max} and ϵ_{max}, as illustrated in Figure 13. The solid line in this figure represents the following equation:

$$W_{adh} = 0.25(\sigma_{max}\epsilon_{max}h_0) \quad (6)$$

The fact that the different experimental results all lie relatively close to a single straight line indicates that the shapes of the different tack curves are similar. In this case the effects of different experimental conditions on σ_{max} and ϵ_{max} can be considered independently when optimizing overall adhesive performance. For example, σ_{max} is often not strongly dependent on the experimental conditions, provided that good bonding is obtained between the substrate and the PSA. In this case the adhesive performance is determined primarily by ϵ_{max}, and the rate dependence of this quantity determines the application window for the adhesive. As described above, the acrylic acid content of the polymer will significantly

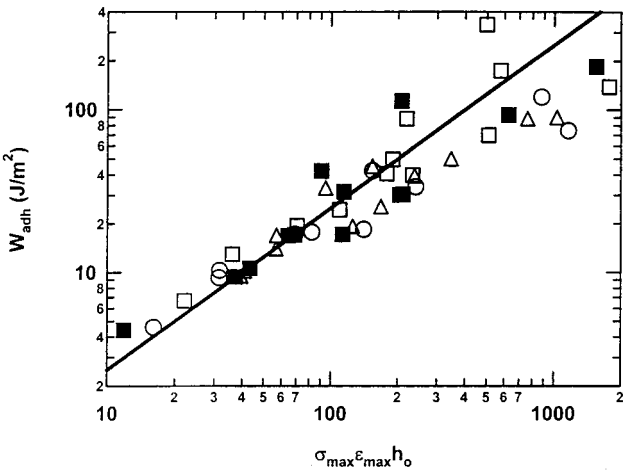

Figure 13. Overall work of adhesion as a function of $\sigma_{max}\epsilon_{max}h_0$ for the PnBA samples: (○) PnBA-AA-100; (□) PnBA-AA-180; (△) PnBA-AA-300. (b) (■) PnBA-M-180. The solid line is the linear relationship given by eq 6.

affect the location of this application window for a monodisperse polymer. The breadth of this application window remains relatively narrow for monodisperse polymers, however.

The narrow application window for monodisperse PSAs is an important practical limitation and arises from the relatively sharp peak in the plots of ϵ_{max} as a function of the Deborah number (Figure 11). A consequence of this behavior is that the optimum molecular weight will depend relatively strongly on the rate and temperature at which the test is performed. Within the range of rates and temperatures investigated in our study, the higher molecular weight polymers (PnBA-AA-860 and PnBA-M-860) are never in the De regime where fibrillation is possible. At the other extreme, very low molecular weight polymers give mechanically unstable fibrils with a low maximum extension. For the polymers with intermediate molecular weights, high values of ϵ_{max} are obtained only over about 1 decade in De, corresponding to a temperature window of 5−10 °C at the most. Furthermore, these high fibril extensions always correspond to cohesive failure, which is not acceptable for many PSA applications, including those where the PSA must be removable.

In comparison, polydisperse materials can give high values of ϵ_{max} over at least 5 decades of debonding rate,[7] corresponding to a useful temperature window of 30−40 °C. Two molecular features of the PEHA adhesives discussed in this previous paper are particularly interesting in practice. First, the presence of chain branching and of a gel fraction causes strain hardening of the fibrils and eventual fibril detachment rather than cohesive fracture. Second, the low molecular weight fraction contributes to the ability of the adhesive to establish good contact with a surface during the bonding portion of the experiment. Therefore, contrary to many polymer applications where mechanical properties are important, a large polydispersity is essential to have the right balance of properties over a practically useful range of temperatures and debonding rates.

5. Summary and Conclusions

We have demonstrated in this study that the debonding process of a soft polymer melt from a solid substrate can be separated into three subprocesses that occur when a tensile stress is applied to the adhesive bond.

In the first subprocess, failure is initiated by the nucleation of cavities at or near the interface between the adhesive and the adherent. The formation of these cavities is associated with the peak in applied stress that is observed in the debonding curve. As long as the terminal relaxation time of the polymer is larger than the characteristic experimental time (De > 1), this cavitation process is essentially controlled by the elastic properties of the adhesive. In this regime the observed maximum stress is proportional to the elastic modulus G' at an effective frequency determined by the imposed debonding velocity. This maximum stress is relatively independent of molecular weight and of the presence of acrylic acid.

The second and third subprocesses correspond to the lateral and extensional growth of these cavities. In monodisperse poly(*n*-butyl acrylates), these two process take place concurrently. The nature of these deformation processes is controlled by an effective Deborah number of the experiment, defined as the temperature-shifted initial strain rate, $a_T V_{deb}/h_0$, multiplied by the terminal relaxation time, τ_d. The value of the Deborah number (De) can be used to separate the behavior of the monodisperse PnBA samples into the following regimes:

(1) De < 10: Lateral and extensional growth of the cavities both occur by viscous flow, but the lateral growth dominates. As a result, the PnBA layer fails cohesively at low strains, giving a low overall adhesion energy.

(2) 10 < De < 1000: Lateral growth is limited, and extensional growth dominates. This is the useful regime for use as a pressure-sensitive adhesive because extensive fibrillation takes place and the dissipated energy is high.

(3) De > 1000: No extensional growth takes place for the carboxylated polymers, and failure occurs adhesively by lateral crack propagation in a manner similar to what would be observed for a cross-linked rubber on a solid surface. Methylation greatly increases the rate at which extensional cavity growth can occur, shifting the transition to adhesive failure to values of De that are approximately 2 orders of magnitude larger. This shift illustrates the important role that acrylic acid groups play in modifying the extensional properties of the polymer.

Two important limitations of monodisperse polymer melts in PSA applications are the very narrow window in Deborah number for useful PSA properties and the absence of strain hardening in elongation. Both can be addressed by using polymers with a broad distribution of relaxation times and with extensive chain branching or light cross-linking.[32,33]

Acknowledgment. We thank Dr. Philippe Kahn for his help in the synthesis of the diazomethane and for the methylation of the PnBA polymers. This collaborative work was partially funded by a NSF−CNRS research grant awarded jointly by the Western Europe Program of the NSF Division of International Programs and by the Direction des Relations Internationales of the CNRS. Acknowledgment is also made to the donors of the Petroleum Research Fund and to the NSF under Grant DMR-9457923 for partial support of this work.

References and Notes

(1) Creton, C. In *Materials Science of Pressure-Sensitive-Adhesives*, 1st ed.; Meijer, H. E. H., Ed.; VCH: Weinheim, 1997; Vol. 18, pp 707−741.
(2) Zosel, A. *Colloid Polym. Sci.* **1985**, *263*, 541−553.
(3) Krenceski, M. A.; Johnson, J. F. *Polym. Eng. Sci.* **1989**, *29*, 36−43.
(4) Zosel, A. *Adv. Pressure Sensitive Adhes. Technol.* **1992**, *1*, 92−127.
(5) Crosby, A. J.; Shull, K. R.; Lakrout, H.; Creton, C. *J. Appl. Phys.* **2000**, *88*, 2956−2966.
(6) Creton, C.; Lakrout, H. *J. Polym. Sci., Part B: Polym. Phys.* **2000**, *38*, 965−979.
(7) Lakrout, H.; Sergot, P.; Creton, C. *J. Adhes.* **1999**, *69*, 307−359.
(8) Crosby, A. J.; Shull, K. R. *J. Polym. Sci., Part B: Polym. Phys.* **1999**, *37*, 3455−3472.
(9) Gay, C.; Leibler. L. *Phys. Rev. Lett.* **1999**, *82*, 936−939.
(10) Kaelble, D. H. *Trans. Soc. Rheol.* **1965**, *9*, 135−163.
(11) Christensen, S. F.; McKinley, G. H. *Int. J. Adhes. Adhes.* **1998**, *18*, 333−343.
(12) Fayt, R.; Forte, R.; Jacobs, C.; Jérôme, R.; Ouhadi, T.; Teyssié, P.; Varshney, S. K. *Macromolecules* **1987**, *20*, 1442−1444.
(13) Varshney, S. K.; Jacobs, C.; Hautekker, J.-P.; Bayard, P.; Fayt, R.; Jérôme, R.; Teyssié, P. *Macromolecules* **1991**, *24*, 4997−5000.
(14) Ahn, D.; Shull, K. R. *Langmuir* **1998**, *14*, 3637−3645.
(15) Klein, J. W.; Gnanou, Y.; Rempp, P. *Polym. Bull.* **1990**, *24*, 39−43.
(16) Arndt, F. *Org. Synth.* **1943**, *2*, 165−167.
(17) Creton, C.; Leibler, L. *J. Polym. Sci., Part B: Polym. Phys.* **1996**, *34*, 545−554.
(18) Hui, C. Y.; Lin, Y. Y.; Baney, J. M. *J. Polym. Sci., Part B: Polym. Phys.* **2000**, *38*, 1485−1495.
(19) Gent, A. N.; Lindley, P. B. *Proc. R. Soc. London, A* **1958**, *249*, 195−205.
(20) Lindsey, G. H. *J. Appl. Phys.* **1967**, *38*, 4843−4852.
(21) Denecour, R. L.; Gent, A. N. *J. Polym. Sci.*, Part *A-2: Polym. Phys.* **1968**, *6*, 1853−1861.
(22) Gent, A. N.; Tompkins, D. A. *J. Appl. Phys.* **1969**, *40*, 2520−2525.
(23) Kaelble, D. H. *Trans. Soc. Rheol.* **1971**, *15*, 275−296.
(24) Gent, A. N.; Wang, C. *J. Mater. Sci.* **1991**, *26*, 3392−3395.
(25) Chikina, I.; Gay, C. *Phys. Rev. Lett.* **2000**, *85*, 4546−4549.
(26) Lin, Y. Y.; Hui, C. Y.; Conway, H. D. *J. Polym. Sci., Part B: Polym. Phys.* **2000**, *38*, 2769−2784.
(27) Maugis, D.; Barquins, M. *J. Phys. D*: *Appl. Phys.* **1978**, *11*, 1989−2023.
(28) Lin, Y. Y.; Hui, C. Y.; Baney, J. M. *J. Phys. D*: *Appl. Phys.* **1999**, *32*, 2250−2260.
(29) Derail, C.; Allal, A.; Marin, G.; Tordjeman, P. *J. Adhes.* **1997**, *61*, 123−157.
(30) Benyahia, L.; Verdier, C.; Piau, J. M. *J. Adhes.* **1997**, *62*, 45−73.
(31) Gent, A. N.; Petrich, R. P. *Proc. R. Soc. London, A* **1969**, *310*, 433−448.
(32) Zosel, A. *Int. J. Adhes. Adhes.* **1998**, *18*, 265−271.
(33) Zosel, A.; Ley, G. *Macromolecules* **1993**, *26*, 2222−2227.

MA0020279